Available online at www.sciencedirect.com
ScienceDirect
Bioorganic & Medicinal Chemistry 16 (2008) 721–731
Bioorganic & Medicinal Chemistry

Eupalinin A isolated from *Eupatorium chinense* L. induces autophagocytosis in human leukemia HL60 cells

Tomohiro Itoh,[a,*] Yuko Ito,[b] Kenji Ohguchi,[a] Masayoshi Ohyama,[c] Munekazu Iinuma,[c] Yoshinori Otsuki,[b] Yoshinori Nozawa[a] and Yukihiro Akao[a]

[a]*Gifu International Institute of Biotechnology, 1-1 Naka-Fudogaoka, Kakamigahara, Gifu 504-0838, Japan*
[b]*Osaka Medical College, 2-7 Daigaku-cho, Takatsuki, Osaka 596-8686, Japan*
[c]*Gifu Pharmaceutical University, 5-6-1 Mitahora-higashi, Gifu 502-8585, Japan*

Received 10 August 2007; revised 10 October 2007; accepted 12 October 2007
Available online 17 October 2007

Abstract—Eupalinin A, a natural phytoalexin included in *Eupatorium chinense* L., exhibited a marked inhibitory effect on cell growth in HL60 cells. The morphological aspects of eupalinin A-treated cells evaluated by Hoechst 33342 nuclear staining indicated cell death, only a small part of which showed a typical apoptosis with nuclear fragmentation and condensation. To determine what type of cell death is caused by eupalinin A, we examined the contribution of caspases, Bcl-2 family proteins, MAP kinase, and PI3K/Akt, and mitochondrial membrane potential to this cell death. As a result, most part of the cell death was not associated with apoptosis because of caspase independence and no death factor released from mitochondria. Electron microscopic study indicated a characteristic finding of autophagy such as the formation of autophagosomes. Furthermore, the level of microctubule-associated-protein light chain 3 (LC3) II protein and monodancylcanaverin (MDC) incorporation were gradually increased with reduction of mitochondrial membrane potential by the accumulation of intracellular ROS after eupalinin A treatment. From these results, we can conclude that eupalinin A-induced cell death was mainly due to autophagy, which was initiated by increased ROS, resulting in the perturbation of mitochondrial membrane potential. Since the class III PI3K inhibitor such as 3-MA or LY294002 did not inhibit the eupalinin A-induced type II programmed cell death (PCD II), it was suggested that the PCD II was executed by Beclin-1 independent pathway of damage-induced mitochondrial autophagy (mitophagy).

1. Introduction

Eupatorium (syn. *Ayapana* Spach) is a genus of flowering plants containing from 36 to 60 species, most of which are herbaceous perennial plants growing to 0.5–3 m tall, but a few are shrubs. The genus is native to temperate regions of the Northern Hemisphere. Species of *Eupatorium* have been used in folk medicine, for instance to excrete uric acid which causes gout, but they also contain toxic compounds that can cause liver damage. Recently, it has been reported that species of *Eupatorium* has antibacterial,[1] anti-inflammatory,[2] anti-oxidant,[2] and antitumor activity.[3,4] Previously, we have obtained several sesquiterpene lactones which were isolated from *Eupatorium chinense* L. and determined the structures of the compounds contained in the fraction. Parthenolide, a major sesquiterpene lactone, has been known to inhibit growth of tumor cells. Especially, bioactive effect of parthenolide is mediated by preventing NF-κB signaling.[5,6] Thus, sesquiterpene lactones may be candidates of cancer preventive agents.

Cell death comprises several types, as evaluated by morphology. Autophagic cell death is an evolutionarily conserved membrane trafficking pathway for the

Abbreviations: DMSO, dimethylsulfoxide; DTT, (±)-dithiothreitol; EDTA, ethylenediamine tetraacetic acid; EGTA, ethylene glycol tetraacetic acid; ERK, extracellular signal-regulated kinase; Hepes, 2-[4-(2-hydroxyethyl)-1-piperazinyl]ethanesulfonic acid; MAPK, mitogen-activated protein kinase; MEK, MAPK/ERK kinase; mTOR, mammalian target of rapamycin; PI3K/Akt, phosphoinositide 3-kinase/Akt; PKA, cAMP-dependent protein kinase; PKC, protein kinase C; PVDF, polyvinylidene fluoride; ROS, reactive oxygen species; TNF-α, tumor necrosis factor-α; Z-VAD-FMK, *N*-benzyloxycarbonyl-Val-Ala-Asp fluoromethylketone.

Keywords: Eupalinin A; Type II programmed cell death; Apoptosis; Autophagy; Sesquiterpene lactone.

* Corresponding author. Tel.: +81 583 71 4646; fax: +81 583 71 4412; e-mail: titoh@giib.or.jp

0968-0896/$ - see front matter © 2007 Elsevier Ltd. All rights reserved.
doi:10.1016/j.bmc.2007.10.033

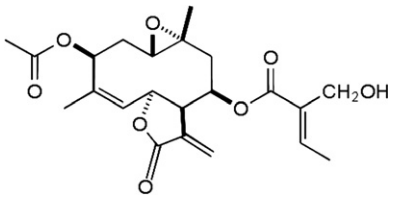

Figure 1. Chemical structure of eupalinin A.

degradation of long-lived proteins and cytoplasmic organelles. Autophagy is characterized by the appearance of double-membrane cytoplasmic vesicles engulfing bulk cytoplasm and/or cytoplasmic organelles such as mitochondria and endoplasmic reticulum (autophagosome). Autophagosome fuses to lysosome to become autolysosome, where sequestered cellular components are digested. In mammalian cells, the formation of the autophagosome is considered to be mediated by phosphoinositide-3-kinase (class III PI3K); its potent inhibitor, 3-methyladenine (3-MA), blocks the formation of autophagosomes. The mammalian autophagy protein, Beclin-1, an orthologue of yeast Atg6, forms a complex with class III PI3K that is responsible for autophagosome formation.

In the present study, we investigated the mechanism of cell death induced by eupalinin A (Fig. 1), one of the sesquiterpene lactones extracted from *Eupatorium chinense* L., in human leukemia HL60 cells and concluded that the cell death was mainly due to type II programmed cell death (PCD II), which was associated with the mitochondrial dysfunction by accumulation of intracellular ROS. Furthermore, it was suggested that eupalinin A-induced PCD II was executed by Beclin-1 independent pathway of damage-induced mitochondrial autophagy (mitophagy).

2. Results

2.1. Eupalinin A-induced growth inhibition and cell death in HL60 cells

We examined eupalinin A for its cytotoxic effect on HL60 cells. Treatment of HL60 cells with eupalinin A inhibited cell growth in a time- and dose-dependent manner (Fig. 2A). The growth of the HL60 cells was markedly suppressed at more than 4 μM, as compared with the control without eupalinin A. We estimated an IC_{50} as 2.4 μM. In the treatment with 4 μM eupalinin A for 24 h, we observed an apparent morphological change, such as nuclear condensation and fragmentation in the cells (Fig. 2B). The nonnucleosomal DNA fragmentation was observed at 1 h after the treatment and the DNA fragmentation was in a time-dependent manner, however, dose-dependency was not observed at 6 h (Fig. 2C). The nucleosomal DNA ladder formation was observed at 2 h but marginal, and neither time- (Fig. 2: left film) nor dose-dependent. Thus, it was suggested that eupalinin A-induced cell death was not necessarily due to apoptosis.

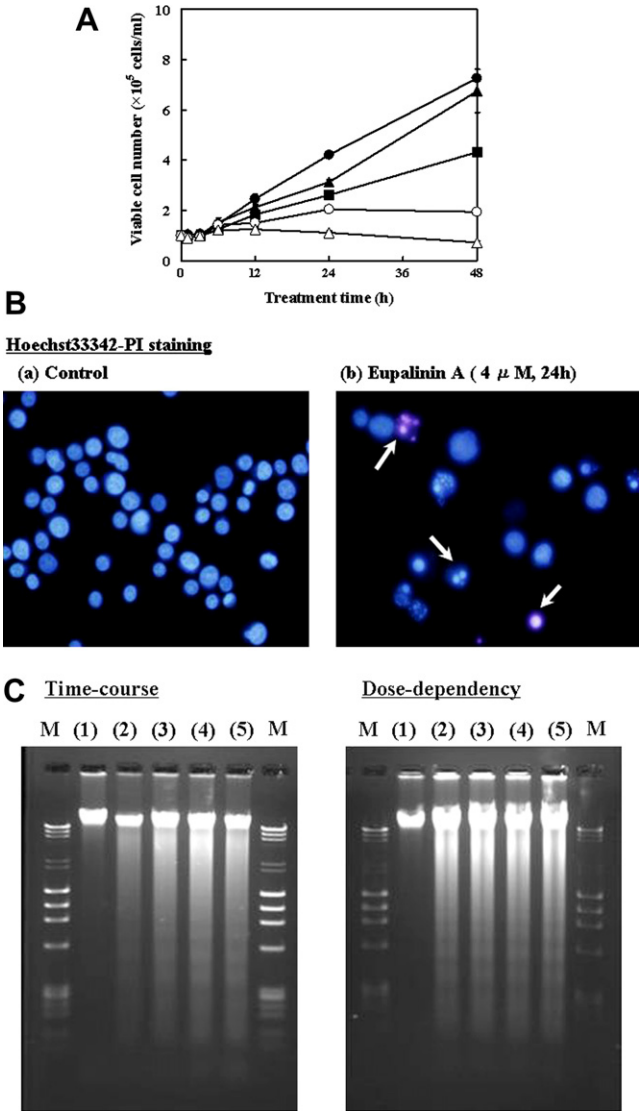

Figure 2. Eupalinin A-induced cell death in HL60 cells. (A) Growth of HL60 cells and its inhibition by eupalinin A. Cells were grown in the absence or presence of 1–8 μM of eupalinin A. ●, control; ▲, eupalinin A (1 μM); ■, eupalinin A (2 μM); ○, eupalinin A (4 μM); △, eupalinin A (8 μM). Data are expressed as means ± SE of three different experiments. (B) Morphological changes in HL60 cells treated with eupalinin A. Cells were stained by Hoechst 33342 and PI (magnification × 400). White arrows indicate apoptotic cells. (C) DNA fragmentation in HL60 cells treated with eupalinin A. Time-course: cells were cultured in the absence of eupalinin A (lane 1) or in the presence of eupalinin A (4 μM) for 1 h (lane 2), 2 h (lane 3), 3 h (lane 4), and 6 h (lane 5). Dose-dependency: cells were cultured for 6 h in the absence of eupalinin A (lane 1) or in the presence of eupalinin A at 1 μM (lane 2), 2 μM (lane 3), 4 μM (lane 4), and 8 μM (lane 5). M indicates DNA size marker.

2.2. Characterization of eupalinin A-induced cell death in HL60 cells

To further investigate the mechanism of eupalinin A-induced cell death, we first examined the caspase activity. Apoptosis is well known to be executed by the cascade activation of initiator caspases such as caspase-8 and executioners such as caspase-3.[7] The caspase-3 activity measured with Caspase Colorimetric Protease Assay

Kit was not increased by the eupalinin A treatment (Fig. 3A). Furthermore, the active forms of caspases-2, -3, -8, and -9 were not detected by Western blotting (Fig. 3B). The cell death evaluated by Trypan-blue dye exclusion test (Fig. 3C) and Hoechst 33342-PI staining (Fig. 3D) was not prevented by the pre-treatment with pan-caspase inhibitor (100 μM of Z-VAD-FMK). These results indicated that the main cause for eupalinin A-induced cell death was not apoptosis.

2.3. Electron microscopic observations of eupalinin A-treated cells

In order to determine the type of cell death caused by eupalinin A, we conducted a transmission electron microscopic study (TEM). As shown in Figure 4C, after the treatment with 4 μM eupalinin A for 6 h, most of cells have AV. The TEM aspects were obviously different from that of apoptosis (Fig. 4B): formation of AV. These findings suggested that eupalinin A-induced cell death is related to autophagy.

2.4. Biochemical evidence for autophagocytosis

In autophagy, starvation signal makes mTOR signaling inactive and then forms isolation membrane in cytosol.[8] These membranes are extended to surround cytosome including organelle and finally forms lipid bilayer autophagosome. In this autophagosome/autolysosome formation stage, microtubule-associated-protein light chain 3 (LC3), the human homologue of *S. cerevisiae* Atg8, is cleaved by the cystein protease Atg4 to leave a conserved glysine residue. Cleaved LC3 is then transiently linked to the Atg7 protein, then to Atg3, and finally to phosphatidylethanolamine.[9] The lipidated LC3 (LC3 II) form is a potential marker of activation of the autophagic pathway. We examined LC3 I (nonlipidated) and LC3 II (lipidated) by Western blotting. In

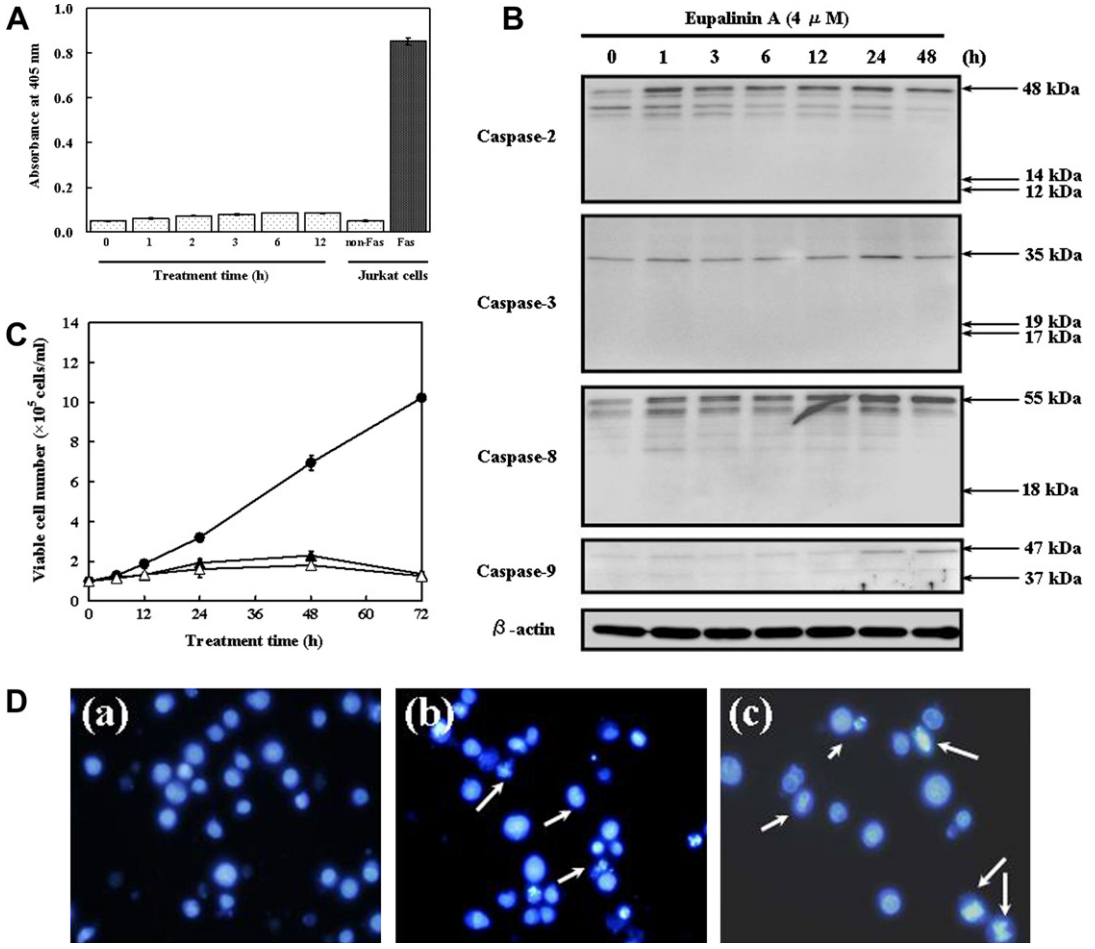

Figure 3. Activities of various caspases and effect of pan-caspase inhibitor (Z-VAD-FMK) on eupalinin A-induced cell death in HL60 cells. (A) Cells were collected at indicated time intervals after 4 μM of eupalinin A treatment and subjected to the caspase-3 activity assay using Caspase Colorimetric Protease Assay Kit. As a positive control, Jurkat cells were treated with or without anti-Fas antibody (CH-11). Data are expressed as means ± SE of three different experiments. (B) Activation of caspase-2, -3, -8, and -9 after the treatment with 4 μM eupalinin A was examined by Western blot analysis. (C) Growth of HL60 cells and its inhibition by eupalinin A or eupalinin A plus pan-caspase inhibitor. Cells were incubated in the presence of 100 μM of the inhibitor. Viable cell number was measured by Trypan-blue dye exclusion test. Data are expressed as means ± SE of three different experiments. ●, control; ▲, eupalinin A (4 μM); △, eupalinin A (4 μM) + Z-VAD-FMK (100 μM). White arrows indicate the apoptotic cells. (D) Morphological changes in HL60 cells treated with DMSO (a), eupalinin A (b), and eupalinin A plus pan-caspase inhibitor for 24 h (c). Cells were stained by Hoechst 33342 and PI (magnification × 400).

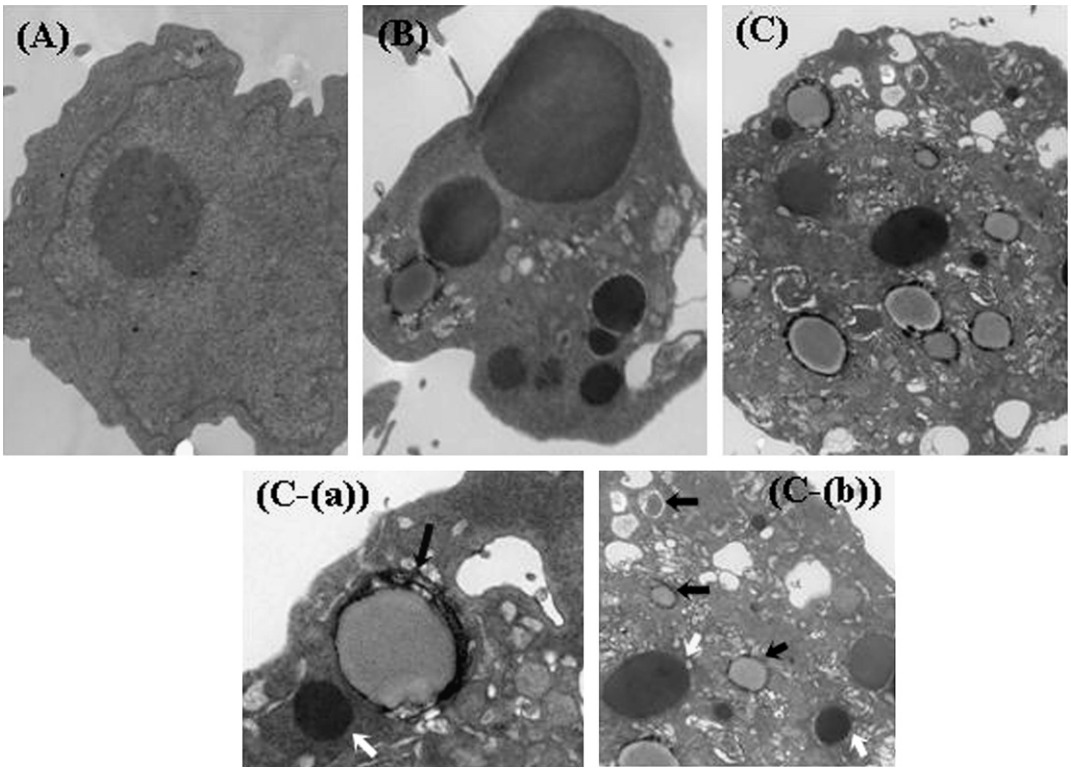

Figure 4. Electron microscopic observations of eupalinin A-treated cells. Cells were examined using TEM. HL60 cells were treated with vehicle control (A) or 4 μM eupalinin A (C) for 6 h. Black arrows indicate autophagosome/autolysosome. White arrows indicate fragmented nuclei (C-a, b). As a morphological feature of apoptotic cell, HL60 cells were treated with actinomycin D (1 μg/ml, 6 h) (B).

addition, to evaluate the formation of autophagosome, we examined MDC staining and measurement of incorporated MDC. As shown in Figure 5A, the level of LC3 II was gradually increased during 3–6 h following the eupalinin A-treatment. When fluorescence microscopic aspects of autophagosomes labeled using MDC in HL60 cells treated with 4 μM eupalinin A were compared with the control cells without eupalinin A treatment, autophagosome formation was significantly elevated at 12 h after the treatment (Fig. 5B,a). MDC incorporation rate was remarkably high at 12 h after treatment (Fig. 5B,b). From these results, eupalinin A-induced cell death was related to PCD II (autophagic cell death). Formation of AV was considered to emerge at 3–6 h after the treatment and terminate by 12 h.

2.5. The relationship between intracellular ROS level and mitochondrial membrane potential, and the expression profile of Bcl-2 family protein, MAPK, and PI3K/Akt signaling in eupalinin A-induced cell death

Recent study reported that mitochondria are a target for the autophagic signal pathway and mitochondrial dysfunction is closely associated with intracellular ROS level.[10] To disclose the relationship between oxidative stress and mitochondrial membrane potential in eupalinin A-induced cell death, we examined intracellular ROS levels using CM-H_2DCF-DA fluorescent probe. As shown in Figure 6A, the intracellular ROS levels were gradually increased during 12 h after the treatment with eupalinin A. On the other hand, the mitochondrial membrane potential was considerably perturbed (Fig. 6B). These results suggested that the increment of intracellular ROS level by eupalinin A links to the reduction of mitochondrial membrane potential. Thus, eupalinin A-induced cell death could be associated with mitochondrial dysfunction. Next, we examined the expression of bcl-2 family protein in eupalinin A-induced cell death. Bcl-2 family proteins have been known to regulate membrane potential and apoptogenic factor (such as, cytochrome *c*, apoptosis inducing factor (AIF), and endonuclease G (Endo G)) release from mitochondria.[11] As shown in Figure 7A, phospho-Bcl 2, Bcl-xl, and phospho-Bad (Ser112, 136) were slightly increased up to 12 h after the treatment, but Bax was slightly decreased. Loss of mitochondrial membrane potential induces release of apoptogenic factors into cytoplasm and decrease of ATP generation, and finally leads to the cell death.[12,13] We examined apoptogenic factors released from mitochondria by Western blot analysis, they were not detected in eupalinin A-treated cells. These results strongly suggested the causal relationship between eupalinin A-induced cell death and mitochondrial dysfunction.

To gain insight into eupalinin A-induced cell death, we investigated the activation of MAP kinase signaling. The MAP kinase signaling pathway plays critical roles in the regulation of cell growth and differentiation.[14–16] There are three well-characterized subfamilies ERK1/2, JNK1/2, and p38 MAP kinase. ERK is activated by phosphorylation by MEK and the MEK/ERK pathway

is involved in apoptosis and survival signaling. In this context, we examined the effect of eupalinin A on MEK and ERK phosphorylation. As shown in Figure 7B, the levels of phospho-MEK and phospho-ERK showed a similar pattern. Phosphorylation of ERK showed a dual pase; increase at 1 h, decrease at 3 h, increase at 6 h after treatment. JNK and p38 MAP kinase are known to be involved in pro-apoptotic signaling. The JNK is preferentially activated by a variety of environmental stresses, including UV and inflammatory cytokines. Eupalinin A appears to elevate the level of JNK and p38 MAP kinase (Fig. 7B).

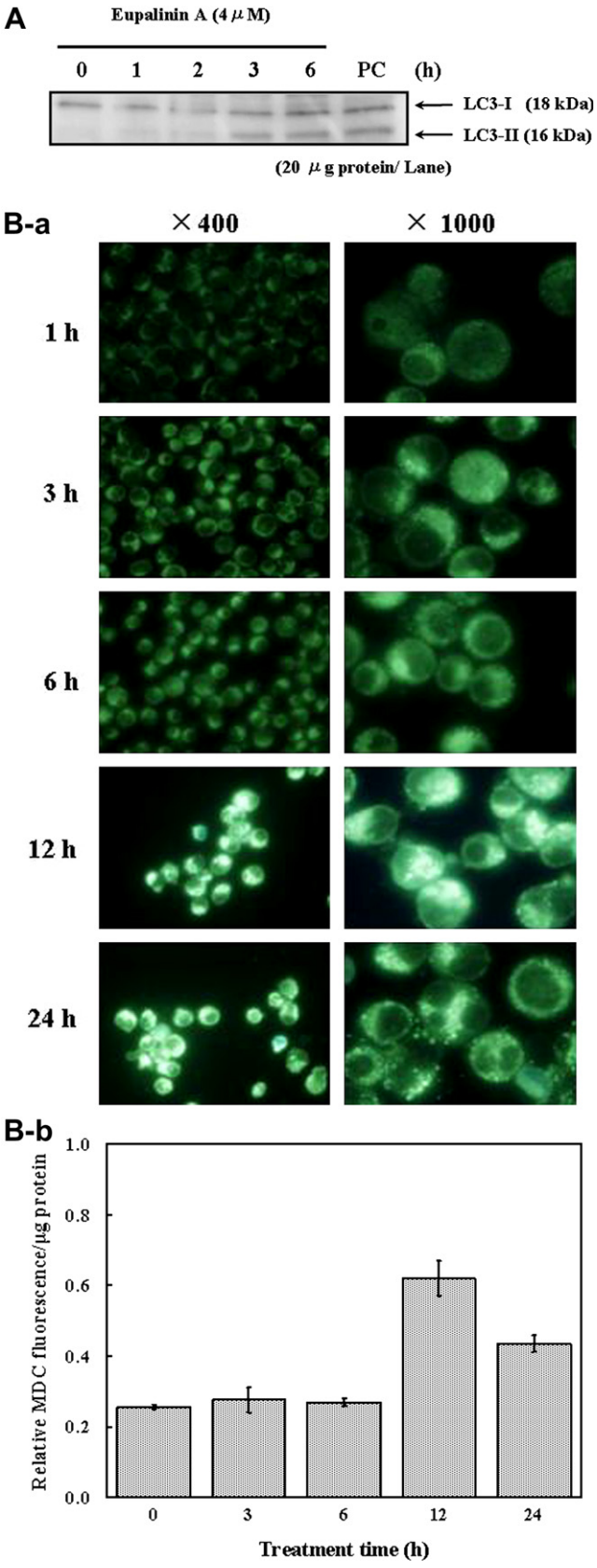

The phosphoinositide 3-kinase (PI3K) pathway has been known to transduce anti-apoptotic signals from a variety of growth and survival factors. The serine/threonine protein kinase Akt is recognized as one of the main downstream effectors of PI3K that promotes cell proliferation and survival.[17,18] When we examined the effect of eupalinin A on Akt phosphorylation, it was shown that Akt activation was increased at 1h after the treatment, which was sustained up to 48 h (Fig. 7C).

2.6. Effect of class III PI3K inhibitors on eupalinin A-induced cell death

To investigate the mechanism whether PI3K is involved in eupalinin A-induced autophagy, cells were treated with eupalinin A in the presence of 3-MA or LY294002. Neither 3-MA nor LY294002 inhibited eupalinin A-induced autophagy (Fig. 8), suggesting that PI3K pathway is not involved in eupalinin A-induced cell death.

3. Discussion

We demonstrated that eupalinin A-induced cell death resulted mainly from type II programmed cell death (PCD II). Evidence for apoptosis was not observed; no involvement of caspase and no death factor released from mitochondria. The DNA fragmentation, which was not nucleosomal, was observed at 1 h in early phase after treatment, thereafter faint DNA ladders appeared. Additionally, only nonnucleosomal DNA fragmentation was increased in a time-dependent manner. From these data, we concluded that eupalinin A-induced cell death was mainly due to PCD II, which was confirmed by transmission electron microscopic observations, MDC staining, and detection of LC3 II protein by Western blot analysis.

In order to disclose the mechanism of autophagy, we first investigated the role of mitochondria in the eupalinin A-induced cell death. In recent study, mitochondria

Figure 5. Eupalinin A-induced autophagy examined by the lipidated LC3 (LCII) form and MDC staining. (A) Immunoblot analysis of LC3 LC3-I (nonlipidated) processing into LC3II (lipidated) in HL60 cells treated with eupalinin A for indicated times. PC; Lyophilized cell lysate from serum starved Neuro 2A cells. (B-a) Mature autophagic vacuoles by eupalinin A treatment (4 μM) were stained by MDC. (B-b) Cells were incubated with 50 μM Monodancylcanaverin (MDC) for 60 min at 37 °C. Intracellular MDC was measured by fluorescence photometry as indicated under Materials and methods. The data represent means ± SE of three different experiments.

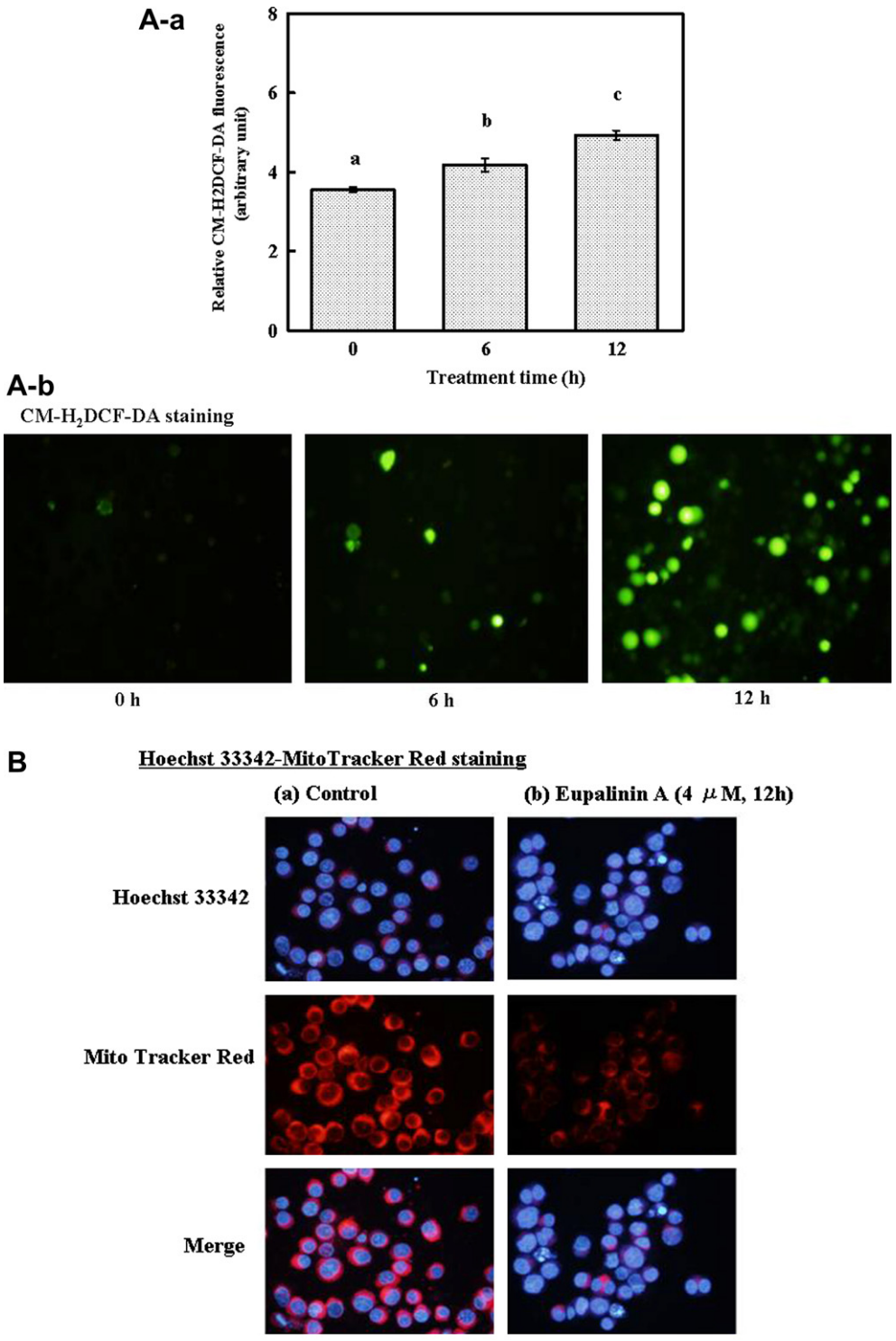

Figure 6. Determination of intracellular ROS levels and perturbation of mitochondrial membrane potential in eupalinin A-induced cells. (A-a) Cells were collected at indicated time intervals after 4 μM of eupalinin A treatment and the intracellular ROS levels measured by incubation with CM-H_2DCF-DA. Data are expressed as means ± SE of three different experiments. (b) The intracellular ROS levels after eupalinin A treatment for 0 h, 6 h, and 12 h were examined by fluorescence microscopy. (B) Mitochondrial membrane potential in HL60 cells treated with eupalinin A. Cells were stained by Mito Tracker Red (magnification × 400).

are a target not only for apoptosis but also for the autophagic pathway.[10] In eupalinin A-induced PCD II, intracellular ROS levels were increased up to 12 h after the treatment, whereas mitochondrial membrane potential was markedly reduced at 12 h. Thus, it was strongly suggested that increased oxidative stress may trigger mitochondrial dysfunction in eupalinin A-induced PCD II. Many reports suggested that, for example,

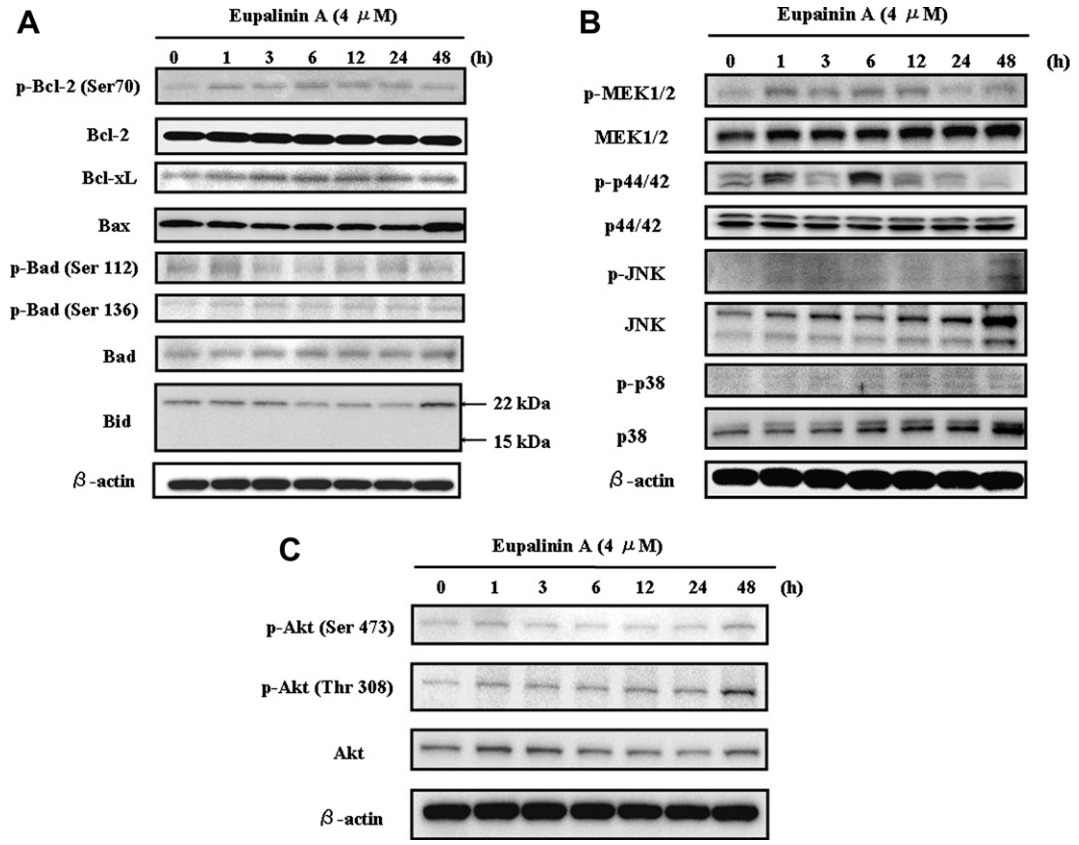

Figure 7. Expression of Bcl-2 family protein, expression profiles of PI3K/Akt and MAPKs in eupalinin A-induced cells. Expression and phosphorylation of Bcl-2 family proteins (A), MAP kinases (B), and PI3K/Akt (C) in eupalinin A (4 μM)-treated HL60 cells were examined by Western blot analysis.

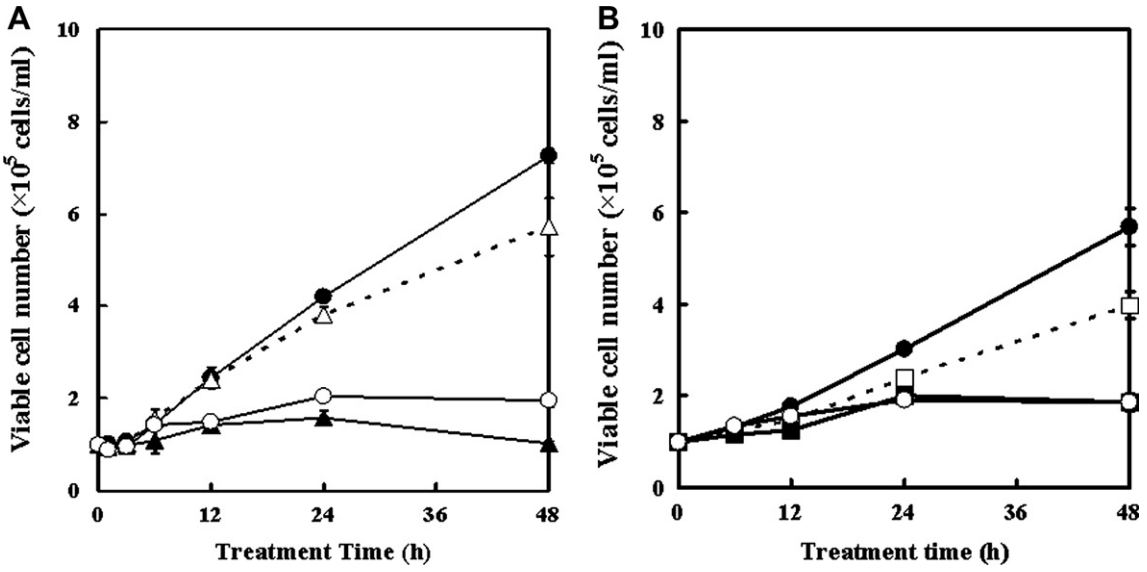

Figure 8. Eupalinin A-induced apoptosis/autophagy was not suppressed by 3-methyladenine (3-MA) or LY294002. HL60 cell proliferation after treatment with vehicle control (●, DMSO), 4 μM eupalinin A (○), 4 μM eupalinin A with 2 mM 3-MA (▲, A) or 2 μM LY294002 (■, B). Dotted line indicates 3-MA (△, 2 mM) or LY294002 (□, 2 μM) alone treatment.

ROS regulates autophagy through redox-sensitive proteases, Atg4.[19–22] Especially, H_2O_2 regulates Atg4 activation. Moreover, the increase of intracellular ROS was caused by the selective autophagic degradation of the major enzymatic ROS scavenger, such as a catalase.[23] Anti-cancer drugs, such as doxorubicin, have been observed to generate intracellular ROS by their metabolites.[24] Eupalinin A also is assumed to generate the intracellular ROS probably by its metabolites. Mitochondria are also implicated in the integration of

apoptotic and autophagic cell death. Lemasters et al. reported that autophagy may block apoptosis by preventing the release of pro-apoptotic mitochondrial factors to the cytoplasm due to the elimination of damaged mitochondria.[25] And mitochondrial damage-induced autophagic cell death may occur especially under conditions where mitochondrial-based apoptosis is not dominant or it is blocked by caspase inhibitors.[26] These findings indicated that mitochondrial function is closely related to cell death (apoptosis and/or autophagy). Thus, it was suggested that mitochondrial dysfunction by accumulation of intracellular ROS was associated with the eupalinin A-induced PCD II.

Phospho-Bcl-2 and Bcl-xl anti-apoptotic proteins were slightly increased by eupalinin A-treatment, which is consistent with the observations reported previously. Recently, Cui et al. reported that increase of phospho-Bcl-2 acts as a suppressive factor of autophagy in oridonin-treated HeLa cells.[27] However, in our study, the increase of phospho-Bcl-2 by eupalinin A treatment promoted the autophagy. Phospho-Bcl-2 suppressed the release of pro-apoptotic factors from mitochondria. This result indicates that the increase of phospho-Bcl-2 level by eupalinin A treatment acts as anti-apoptotic event (survival). On the other hand, apoptosis is induced when Bcl-xl binds to Bad.[28–32] The expression level of Bad, which is pro-apoptotic Bcl-2 family protein, is regulated by the signaling pathways such as ERK 1/2, Akt, PKC, and PKA.[33–37] In apoptosis, the phospho-Bad (Ser112, 136) interacts with 14-3-3 protein, resulting in the suppression of binding of Bcl-xl and Bcl-2 at mitochondria. In the current study, the levels of phospho-Bad (Ser112, 136) were increased at 1 h and Bcl-xl was increased from 1 h up to 12 h. Importantly, phospho-ERK1/2 level was increased at 1h after the treatment. These results suggested that the activation of ERK 1/2 links to the activation of Bad. Apoptosis signal-regulating kinase 1 (ASK1), which regulates the action of JNK, is phosphorylated by Akt.[38,39] However, our data showed no significant changes in the levels of phospho-Akt and phospho-ASK1 protein. Lenardo et al. had reported that autophagic cell death of L929 cells is dependent on JNK.[40] And the receptor-interacting protein (RIP), a protein associated with the cytoplasmic domain of death receptor, and the activation of JNK and its upstream kinase, MKK7, are involved in the accumulation of autophagic vacuoles.[41] Another report has also shown that the autophagic cell death was implicated in c-Jun that is a target factor of JNK.[41] In our study, since the activated JNK level was very low, the participation of JNK may be marginal in eupalinin A-induced autophagy. Further study to clarify the relationship of JNK and p38 MAP kinase with autophagy is needed. Moreover, Bax, pro-apoptotic protein, was slightly decreased while Bcl-xl was increased by the treatment. Many reports have suggested that apoptosis execution is associated with the balance between Bcl-2/Bcl-xl and Bax/Bak.[42] Mizushima et al. reported that Bcl-2 anti-apoptotic proteins inhibit Beclin 1-dependent autophagy.[43] In our experiment, since the level of Bcl-2 was not changed by eupalinin A. It was assumed that eupalinin A-induced PCD II was not associated with Beclin 1-dependent autophagy pathway. In fact, when we have treated with eupalinin A and 3-MA or LY294002, which were autophagy inhibitors, eupalinin A-induced cell death was not prevented (Fig. 8). Furthermore, the increased level of Bcl-xl and concurrent decrease of Bax suggested that eupalinin A stimulates the signaling of survival rather than apoptosis.

Recent study indicated that NF-κB activation repressed TNF-α-induced autophagy.[44] A sesquiterpene lactone, parthenolide, has been shown to inhibit NF-κB signaling.[5,6] Since phosphorylated IκB, which is a key regulator of NF-κB, was unchanged (data not shown), eupalinin A-induced PCD II was not mediated via NF-κB signaling.

In summary, eupalinin A-induced cell death was mainly due to PCD II, which was associated with mitochondria dysfunction induced by the increase of intracellular ROS, and anti-apoptotic signals. However, further study is required to clarify the relationship between oxidative stress and the signaling responsible for autophagy induced by eupalinin A. With respect to the relationship between apoptosis and autophagy, we could observe weak oligonucleosomal DNA fragmentation in the early phase, but it did not change with time. Therefore, it was suggested that apoptosis and autophagy were executed independently and thereafter, autophagy was performed because anti-apoptosis signal becomes predominant. Several reports indicated that apoptosis and autophagy may be interconnected.[40,43,45,46] It was reported that proteins like death-associated protein kinase (DAPk) and DAPk related protein kinase-1 (DRP-1) promote death in a way that depends on their kinase activities.[47] DAPk predominantly activates apoptosis through a caspase-dependent pathway.[48] But, in mouse embryonic fibroblasts in which apoptosis cannot be activated, DAPk and DPR-1 instead induce autophagy.[49] Therefore, it is assumed that DAPk and DRP-1 are playing a role of switching of apoptosis/autophagy signal. However, the mechanism of this switching between apoptosis and autophagy is currently obscure. It remains, therefore, what determines the type of cell death induced by eupalinin A.

Recently, natural products, such as resveratrol,[50] oridonin,[51] and soy bean B-group triterpenoid saponins,[52] induced autophagic cell death. These substances mediated Beclin-1 dependent autophagy. But in our study, eupalinin A-induced autophagy was executed by Beclin-1 independent pathway of damage-induced mitochondrial autophagy (mitophagy). Eupalinin A and the extracts which contain it will be expected as anti-neoplastic agents through the autophagic machinery that is different from soy bean saponin and oridonin.

4. Materials and methods

4.1. Materials

Eupalinin A used in this study was separated by column chromatography, and identified by ^{1}H, ^{13}C NMR and

Mass spectra. The 25× Complete®, a mixture of protease inhibitors, was obtained from Roche (Penzberg, Germany). The phosphatase Inhibitor Cocktail® 1 and 2 was from Sigma (St. Louis, MO, USA). The antibodies to anti-human MEK1/2, anti-human phospho-MEK1/2 (Ser217/221), anti-human p44/42 MAP Kinase (ERK), anti-human phospho-p44/42 MAPK (Thr202/Tyr204) (p-ERK), anti-human SAPK/JNK (JNK), anti-human phospho-SAPK/JNK (Thr183/Tyr185) (p-JNK), anti-human p38 MAP kinase (p38), anti-human phospho-p38 MAP Kinase (Thr180/Tyr182) (p-p38), anti-human Bad, anti-human phospho-Bad (Ser112, Ser 136) (p-Bad), anti-human Bid, and anti-human phospho-IκB-α (Ser32/36) (p-IκB) were from Cell Signaling Technology (MA, USA). The antibodies to anti-human caspase-3 and anti-human Bcl-xL (H-5) were from Santa Cruz Biotechnology (CA, USA). The antibodies to anti-human caspase-2, anti-human caspase-8, and anti-human caspase-9 were from MBL (Nagoya, Japan). The antibodies to anti-human endonuclease G and anti-human ß-actin were from Sigma. The antibody to anti-human AIF was from ProSci Inc (CA, USA). The antibody to anti-human cytochrome *c* was from Upstate Biotechnology (NY, USA). The antibody to LC-3 was from Nano Tools antikoerpertechnik (Teningen, Freiburg, Germany). Anti-rabbit and anti-mouse antibodies conjugated with horseradish peroxidase and the chemiluminescence (ECL) kit were obtained from GE Healthcare Sci. (Amersham Place, Little Chalfont, Buckinghamshire, HP7 9NA, England). The other reagents were of the highest quality available.

4.2. Cell culture and treatment

Human M2-type leukemia cell line HL60 was provided by RIKEN Cell Bank (Tsukuba, Ibaraki, Japan). HL60 cells were cultured in RPMI-1640 medium (Invitrogen, Carlsbad, CA, USA) supplemented with 10% heat-inactivated fetal bovine serum (FBS). Eupalinin A dissolved in DMSO was added to the cell culture with final concentration of DMSO (<0.3%) that showed no significant effect on the growth and differentiation of HL60 cells (data not shown). Viable cell number was measured by Trypan-blue dye exclusion test using a Burker–Turk type cell count chamber.

4.3. Morphological change in HL60 cells

For the morphological examination of cell death, the cells were double-stained with Hoechst 33342 (Calbiochem, Sandiego, CA, USA) and Propidium iodide (PI) (Molecular Probes). Hoechst 33342 and PI were added to the cultured medium at a concentration of 5 μg/ml. After incubation for 30 min, the cells were collected and washed with phosphate-buffered saline (PBS) and then observed under a fluorescence microscope, Olympus BX-50 (Olympus, Tokyo, Japan).

4.4. DNA extraction and agarose gel electrophoresis

The cultured cells were treated with eupalinin A and the control cells were treated with DMSO alone. The cells were collected and washed with PBS. Lysis buffer (100 mM Tris–HCl (pH 7.4), 5 mM EDTA, 200 mM NaCl, 0.2% SDS, and 200 μg/ml Proteinase K (Takara, Ohtsu, Shiga, Japan)) was added to the cell pellet and incubated at 55 °C for 3 h. After incubation, DNA was extracted with phenol/chloroform from the cell lysate. DNA was precipitated with ethanol and dissolved with Tris–EDTA buffer. RNase A (Sigma) was added to the DNA solution at a final concentration of 20 μg/ml. DNA (3 μg) was analyzed by electrophoresis on 2% agarose gel.

4.5. Electron microscopic observation

The cells treated or untreated with eupalinin A (4 μM) were harvested and rinsed with PBS. Cells were fixed for 30 min in 4% paraformaldehyde and 1% glutaraldehyde in 0.1 M phosphate buffer (pH 7.4) (PB), rinsed in PB, and postfixed in 1% osmium tetraoxide for 30 min. After washing with PB, cells were progressively dehydrated in a 10% graded series of 50–100% ethanol and then cleared in QY-1 (Nissin EM, Tokyo, Japan). Cells were embedded in Epon 812 resin (TAAB Laboratories Equipment, Reading, UK), and thin sections (70 nm thickness) were stained with uranyl acetate and lead citrate, and then examined by transmission electron microscopy, Hitachi-7650 (Hitachi, Tokyo, Japan), operating at 80 kV.

4.6. Measurement of autophagy

Autolysosome and/or autophagosome (AV) were identified by Munafo et al.'s method.[53,54] For visualization of AV, cells were incubated with 50 μM Monodancylcadaverin (MDC) (Sigma) for 60 min, at 37 °C. After incubation cells were washed twice with PBS and immediately observed under fluorescence microscope (356 nm excitation filter and 545 nm barrier filter). Moreover, MDC treated cells were washed twice with PBS and lysed with RIPA buffer. Intracellular MDC was measured by fluorocount microplate reader (excitation wavelength 360 nm, emission wavelength 530 nm). To normalize the measurements to the number of cells present in each well, protein content of lysate was measured with a DC Protein assay kit.

4.7. Measurement of intracellular ROS level by CM-H_2DCF-DA fluorescent probe

Amount of intracellular ROS was measured by using 5-(and-6-)-carboxy-2′,7′-dichlorodihydrofluorescein diacetate (CM-H_2DCF-DA). CM-H_2DCF-DA is a fluorogenic freely permeable tracer specific for ROS assessment. It is diacetylated by intracellular esterases to the nonfluorescent 2′,7′-dichlorohydrofluorescein (DCFH), which is oxidized to the fluorescent compound 2′,7′-dichlorofluorescein (DCF) by ROS. HL60 cells were incubated with 10 μM CM-H_2DCF-DA for 30 min at 37 °C after eupalinin A treatment. Cells were washed twice with PBS to remove the excess of CM-H_2DCF-DA and were placed on slide glasses and mounted. Photomicrographs of the mounted cells were taken with a fluorescent microscope equipped with UV supply system (Olympus BX-50). Cells stained with CM-H_2DCF-DA

were incubated with 100 μl of lysis buffer for 5 min on ice and then measured with excitation at 490 nm and emission at 530 nm with a fluorometer (MTP-600F, CORONA ELECTRIC Co. Ltd. Hitachinaka, Japan). The level of ROS was expressed as an arbitrary unit of relative value.

4.8. Measurement of mitochondrial membrane potential by Mito-Tracker probe

Mitochondrial membrane potential was measured by use of fluorescent dye, Mito-Tracker Red (Molecular Probes), which accumulates selectively in active mitochondria and becomes fluorescent when oxidized. Mito-Tracker Red was added to cultured medium at a concentration of 10 nM. After the cells were treated with Mito-Tracker Red and washed twice with PBS, the cells were resuspended with PBS and observed under fluorescence microscope.

4.9. Antibodies and Western blotting

For preparation of cell lysate, HL60 cells were washed twice with PBS and harvested. The cell pellet was resuspended in lysis buffer A (2 × PBS, 0.1% SDS, 1% Nonidet P-40, 0.5% sodium deoxycholate, and 25× Complete®) was used to analyze caspase-2, -3, -8, -9, and BID. Lysis buffer B (250 mM sucrose, 20 mM Hepes–KOH (pH 7.5), 10 mM KCl, 1.5 mM $MgCl_2$, 1 mM EDTA, 1 mM EGTA, 1 mM DTT, and 25× Complete®) was used to analyze AIF, cytochrome *c*, Smac/Diablo, and endonuclease G. Lysis buffer C (250 mM sucrose, 20 mM Hepes–KOH (pH 7.5), 10 mM KCl, 1.5 mM $MgCl_2$, 1 mM EDTA, 1 mM EGTA, 1 mM DTT, 1% Nonidet P-40, 25× Complete®, and Phosphatase Inhibitor Cocktail® 1 and 2) was used to analyze MAP kinases, p-IκB, Bad, p-Bad (Ser112, 136), and Bcl-xL. The mitochondrial and cytosolic fractions were prepared as reported previously.[55] Protein content was measured with a DC Protein assay kit (Bio-Rad, Hercules, CA). Five micrograms of protein of each cell lysate was separated by SDS–PAGE by using an adequate percent of polyacrylamide in the gel and electroblotted onto a PVDF membrane (Du Pont, Boston, MA). After blockage of nonspecific binding sites for 1 h by 5% nonfat milk in TPBS (PBS and 0.1% Tween 20), the membrane was incubated overnight at 4 °C with various antibodies. The membrane was then washed three times with TPBS, incubated further with alkaline phosphatase-conjugated goat anti-mouse antibody or anti-rabbit antibody at room temperature, and then washed three times with TPBS. Proteins were detected with enhanced ECL kit and chemiluminescence detector (LAS-1000, Fuji, Japan).

4.10. Effect of class III PI3K inhibitors on eupalinin A-induced type II programmed cell death

HL 60 cells (1×10^5 cells/ml) were pre-treated with 4 mM of 3-MA or 2 μM of LY294002 for 1 h. After pretreatment, eupalinin A was added to cultured medium at a concentration of 4 μM and then incubated for 48 h. The treated cells were subjected to measurement of viable cell number, Hoechst 33342-PI and MDC staining, and MDC incorporation by the above-mentioned method.

5. Conclusion

The data presented here strongly suggested that eupalinin A-induced cell death is mainly due to type II programmed cell death (PCD II). It is to be noted that anti-apoptosis signal and oxidative stress are implicated in the autophagic cell death. Furthermore, eupalinin A-induced PCD II was accompanied with various changes of signaling in the early phase. Switching of autophagy/apoptosis is determined by autophagy/apoptosis singal balance. Therefore, it is necessary to identify the factors which regulate the balance of apoptosis signal and autophagic signaling in an early phase. Further studies are needed to examine the precise interaction of eupalinin A with the autophagy-related signaling.

References and notes

1. Sasikumar, J. M.; Doss, A. P.; Doss, A. *Fitoterapi* **2005**, *76*, 240–243.
2. de las Heras, B.; Slowing, K.; Bendi, J.; Catretero, E.; Ortega, T.; Toledo, C.; Bremejo, P.; Iglesias, I.; Abad, M. J.; Gomez-Serranillos, P.; Liso, P. A.; Villar, A.; Chiriboga, X. *Ethnopharmacology* **1998**, *61*, 161–166.
3. Yan, S. P.; Huo, J.; Wang, Y.; Lou, L. G.; Yue, J. M. *J. Nat. Prod.* **2004**, *67*, 638–643.
4. Shen, Y. C.; Lo, K. L.; Kuo, Y. H.; Khalil, A. T. *J. Nat. Prod.* **2005**, *68*, 745–750.
5. Hehner, S. P.; Henrich, M. H.; Bork, P. M.; Vogt, M.; Ratter, F.; Lehmann, V.; Schulze-Osthoff, K.; Dröge, W.; Schmitz, M. L. *J. Biol. Chem.* **1998**, *16*, 1288–1297.
6. Yip-Schneider, M. T.; Nakshatri, H.; Sweeney, C. J.; Marshall, M. S.; Wiebke, E. A.; Schmidt, C. M. *Mol. Cancer Ther.* **2005**, *4*, 587–594.
7. Thornbery, N. A.; Rano, T. A.; Peterson, E. P.; Rasper, D. M.; Timkey, T.; Garcia-Calvo, M.; Houtzager, V. M.; Nordstorm, P. A.; Roy, S.; Vaillancourt, J. P.; Chapman, K. T.; Nicholson, D. W. *J. Biol. Chem.* **1997**, *18*, 17907–17911.
8. Yorimitsu, T.; Klionsky, D. J. *Cell Death Differ.* **2005**, *12*, 1542–1552.
9. Kabeya, Y.; Mizushima, N.; Ueno, T.; Ymamamotu, A.; Kirisato, T.; Noda, T.; Kominami, E.; Ohsumi, Y.; Yoshimori, T. *EMBO J.* **2000**, *19*, 5720–5728.
10. Elmore, S. P.; Qian, T.; Grissom, S. F.; Lemasters, J. J. *FASEB J.* **2001**, *15*, 2286–2287.
11. Tsujimoto, Y. *J. Cell Physiol.* **2003**, *195*, 158–167.
12. Arnoult, D.; Parone, P.; Martinou, J. C.; Antonsson, B.; Estaquier, J.; Ameisen, C. J. *J. Cell Biol.* **2002**, *159*, 923–929.
13. Uren, R. T.; Dewson, G.; Bonzon, C.; Lithgow, T.; Newmeyer, D. D.; Kluck, R. M. *J. Biol. Chem.* **2005**, *280*, 2266–2274.
14. Raingeaud, J.; Gupta, S.; Rogers, J. S.; Dickens, M.; Ulevitch, R. J. *J. Biol. Chem.* **1995**, *270*, 7420–7426.
15. Lewis, T. S.; Shaprio, P. S.; Ahn, N. G. *Adv. Cancer Res.* **1998**, *74*, 49–139.
16. Weston, C. R.; Davis, R. J. *Curr. Opin. Genet. Dev.* **2002**, *12*, 14–21.
17. Cantley, L. C. *Science* **2002**, *296*, 1655–1657.

18. Vivanco, I.; Sawyers, C. L. *Nat. Rev. Cancer* **2002**, *2*, 489–501.
19. Liu, Z.; Lenardo, M. J. *Dev. Cell.* **2007**, *12*, 484–485.
20. Zhang, Y.; Qi, H.; Taylor, R.; Xu, W.; Liu, L. F.; Jin, S. *Autophagy* **2007**, *3*, 337–346.
21. Scherz-Shouval, R.; Shvets, E.; Fass, E.; Shorer, H.; Elazar, Z. *EMBO J.* **2007**, *26*, 1749–1760.
22. Yan, Y. Q.; Zhang, B.; Wang, L.; Xie, Y. H.; Peng, T.; Bai, B.; Zhou, P. K. *Cancer Lett.* **2007**, *252*, 280–289.
23. Yu, L.; Wan, F.; Dutta, S.; Welsh, S.; Liu, Z.; Freundt, E.; Baehrecke, E. H.; Leonardo, M. *Proc. Natl. Acad. Sci. U.S.A.* **2006**, *103*, 4952–4957.
24. Wanger, B. A.; Evig, C. B.; Reszka, K. J.; Buettner, G. R.; Burns, C. P. *Arch. Biochem. Biophys.* **2005**, *440*, 181–190.
25. Lemasters, J. J.; Nieminen, A. l.; Qian, T.; Trost, L. C.; Elmore, S. P.; Nishimura, Y.; Crowe, R. A.; Cascio, W. E.; Bradham, C. A.; Barnner, D. A.; Herman, B. *Biochim. Biophys. Acta* **1998**, *1366*, 177–196.
26. Gozuacik, D.; Kimchi, A. *Oncogene* **2004**, *23*, 2891–2906.
27. Cui, Q.; Tashiro, S.; Onodera, S.; Ikejima, T. *J. Pharmacol. Sci.* **2006**, *101*, 230–239.
28. Yang, E.; Zha, J.; Jockel, J.; Boise, L. H.; Thompson, C. B.; Korsmeyer, S. J. *Cell* **1995**, *80*, 285–291.
29. Zha, J.; Harada, H.; Yang, E.; Jockel, J.; Korsmeyer, S. J. *Cell* **1996**, *87*, 619–628.
30. Zha, J.; Harada, H.; Osipov, K.; Jockel, J.; Waksman, G.; Korsmeyer, S. J. *J. Bio.l Chem.* **1997**, *272*, 24101–24104.
31. Datta, S. R.; Katsov, A.; Hu, L.; Petos, A.; Fesik, S. W.; Yaffe, M. B. *Mol. Cell.* **2000**, *6*, 41–51.
32. Tan, Y.; Demeter, M. R.; Ruan, H.; Comb, M. J. *J. Biol. Chem.* **2000**, *275*, 25865–25869.
33. del Peso, L.; Gonzalez-Garcia, M.; Page, C.; Herrera, R.; Nunez, G. *Science* **1997**, *278*, 687–689.
34. Datta, S. R.; Dudek, H.; Tao, X.; Masters, S.; Fu, H.; Gotoh, Y.; Greenberg, M. E. *Cell* **1997**, *91*, 231–241.
35. Tan, Y.; Ruan, H.; Demeter, M. R.; Comb, M. J. *J. Biol. Chem.* **1999**, *274*, 34859–34867.
36. Harada, H.; Becknell, B.; Wilm, M.; Mann, M.; Huang, L. J.; Taylor, S. S.; Scott, J. D.; Korsmeyer, S. J. *Mol. Cell.* **1999**, *3*, 414–422.
37. Lizcano, J. M.; Morrice, N.; Cohen, P. *Biochem. J.* **2000**, *349*, 547–557.
38. Kanamoto, T.; Mota, M.; Takeda, K.; Rubin, L. L.; Miyazono, K.; Ichijo, H.; Bazenet, C. E. *Mol. Cell Biol.* **2000**, *20*, 196–204.
39. Zhang, R.; Al-Lamki, R.; Bai, L.; Streb, J. W.; Miano, J. M.; Bradley, J.; Min, W. *Circ. Res.* **2004**, *94*, 1483–1491.
40. Yu, L.; Alva, A.; Su, H.; Dutt, P.; Freundt, E.; Welsh, S.; Baehrecke, E. H.; Lenardo, M. J. *Science* **2004**, *304*, 1500–1502.
41. Codogno, P.; Meijer, A. J. *Cell Death Differ.* **2005**, *12*, 1509–1518.
42. Tsujimoto, Y.; Shimizu, S. *Cell Death Differ.* **2005**, *12*, 1528–1534.
43. Pattingre, S.; Tassa, A.; Qu, X.; Garuti, R.; Liang, X. H.; Mizushima, N.; Parker, M.; Schneider, M. D.; Levine, B. *Cell* **2005**, *122*, 927–939.
44. Djavaheri-Mergny, M.; Amelotti, M.; Mathieu, J.; Besancon, F.; Bauvy, C.; Souquere, S.; Pierron, G.; Codogno, P. *J. Biol. Chem.* **2006**, *41*, 30373–30382.
45. Boya, P.; Gonzalez-Polo, R. A.; Casares, N.; Perfettini, J. L.; Dessen, P.; Larochette, N.; Metivier, D.; Meley, D.; Souquere, S.; Yoshimori, T.; Pierron, G.; Codogno, P.; Kroeemer, G. *Mol. Cell Biol.* **2005**, *25*, 1025–1040.
46. Pyo, J. O.; Jang, M. H.; Kwon, Y. K.; Lee, H. J.; Jun, J. I.; Woo, H. N.; Cho, D. H.; Choi, B.; Lee, H.; Kim, J. H.; Mizushima, N.; Ohsumi, Y.; Jung, Y. K. *J. Biol. Chem.* **2005**, *280*, 20722–20729.
47. Shintani, T.; Klionsky, D. J. *Science* **2004**, *306*, 990–995.
48. Raveh, T.; Droguett, G.; Horwits, M. S.; DePinho, A. R.; Kimchi, A. *Nat. Cell Biol.* **2001**, *3*, 1–7.
49. Inbal, B.; Bialik, S.; Sabanay, I.; Shani, G.; Kimchi, A. *J. Cell Biol.* **2002**, *157*, 455–468.
50. Opipari, A. W.; Tan, L.; Botano, A. E.; Sorenson, D. R.; Aurora, A.; Liu, J. R. *Cancer Res.* **2004**, *64*, 696–706.
51. Cui, Q.; Tashiro, S.; Onodera, S.; Minami, M.; Ikejima, T. *Biol. Pharm. Bull.* **2007**, *30*, 859–864.
52. Ellington, A. A.; Berhow, M.; Singletary, K. W. *Carcinogenesis* **2005**, *26*, 159–167.
53. Biederbick, A.; Kern, H. F.; Elsässer, H. P. *Eur. J. Cell Biol.* **1995**, *66*, 3–14.
54. Munafo, D. B.; Colombo, M. I. *J. Cell Sci.* **2001**, *114*, 3619–3629.
55. Akao, Y.; Otsuki, Y.; Kataoka, S.; Kataoka, S.; Ito, Y.; Tsujimoto, Y. *Cancer Res.* **1994**, *54*, 2468–2471.